



Mechanical and Bionic Structure Characteristics of Clamp-grip and Web-claw Suction Cup Submersible Pipeline Robot

Zhijing Zhou^{1,*}, Gang Yin^{1,2}, Jiachen Zhou³, Yongxiang Zhang¹, Fengzhang Wu¹

¹Zhejiang Haozhonghao Health Products Co., Ltd., Wenzhou, Zhejiang, China.

²Xiangshan Marine Science and Technology Talent Park, Xiangshan, Ningbo, Zhejiang, China.

³Hainan University, Haikou, Hainan, China.

How to cite this paper: Zhijing Zhou, Gang Yin, Jiachen Zhou, Yongxiang Zhang, Fengzhang Wu. (2024) Mechanical and Bionic Structure Characteristics of Clamp-grip and Web-claw Suction Cup Submersible Pipeline Robot. *Engineering Advances*, 4(2), 86-92.
DOI: 10.26855/ea.2024.04.003

Received: March 20, 2024

Accepted: April 17, 2024

Published: May 14, 2024

***Corresponding author:** Zhijing Zhou, Zhejiang Haozhonghao Health Products Co., Ltd., Wenzhou, Zhejiang, China.

Abstract

With the rapid development of modern society, cities have become increasingly dependent on infrastructure such as natural gas and air conditioning pipelines. At the same time, advances in key industries such as oil, chemicals, and nuclear have made pipelines an important bridge between homes and cities, as well as between continents. With the increasing complexity of pipeline systems, the need for pipeline maintenance and repair has become more urgent. In order to solve this problem, the in-tube robot technology has emerged and has been extensively researched and developed in practical applications. Especially in unique working environments like offshore drilling platforms, in-pipe robots must possess robust vertical walking capabilities while also meeting stringent waterproofing and anti-static requirements. These harsh conditions are necessary to ensure the robot operates stably in a complex environment, guaranteeing absolute safety and reliability. The development of in-pipe robot technology can be considered a significant assurance for the safe operation of pipeline systems in modern society.

Keywords

Pipeline robot, webbed claw sucker, rudder, fist-grip structure, micro-probe mechanism

Introduction

With the continuous evolution of in-pipe robot technology, its types have been extended to as many as eight [1], such as wheeled, tracked and peristaltic, etc. However, in the pipeline operation, the robot can move vertically and carry equipment, and the abdominal wall robot is particularly good performance. The pipe-gripping robot described in this paper [2] is a creative design scheme in this field. Our research on gripping and web-claw sucker-like in-pipe robots aims to bring new enlightenment to the research and development of related fields. The gripping crawling mechanism is especially suitable for vertical walking in steel pipe, and the webbed claw sucker is a further development of it, which provides another effective solution for vertical walking in plastic pipe.

1. The special claw grip structure design of the pliers and the specific shape of the claw body

When the claws of the pipeline robot come into contact with the inner wall of the pipeline, due to the special way of deep cutting of the claw teeth, the mechanical analysis of the clamp claw grip structure becomes complicated and is not limited to simple friction analysis. This is because the steel wall of the pipe has extremely high roughness (*i.e.* larger Ra Value), and

even there may be irregular phenomena such as nodules and turbidity pits on the surface. Therefore, its anti-skid performance is closely related to the peak Rz of pipeline roughness, the average Ra of pipeline roughness, and the pressure N exerted by the clamp body Closely related.

For the convenience of explanation, we have introduced a new calculation method in this case, that is, "Clamping slip force" The calculation is used to evaluate the force generated when the claw teeth are in high contact with the inner wall of the pipe. Therefore, the anti-slip effect of the clamp body is actually the result of the combined action of the clamp-in Slip Force F_a and the positive pressure friction resistance F_b . Next, we performed a qualitative micro-mechanistic force analysis of the embedded slippage force mode, where the externally applied load force is defined as F_s and the reaction generated at the peak of the rough surface is defined as F_c , see Figure 1:

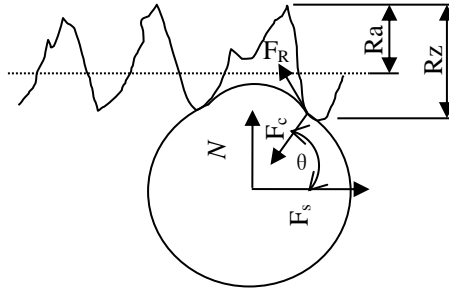


Figure 1. Mechanical force diagram of claw teeth acting on the inner surface of the pipe.

In an ideal plane contact, when external gravity F_s is applied, all the positive pressure N is completely converted into friction, which is only related to the coefficient of friction μ to balance the external gravity, the relation can be expressed as $F_s = F_b = \mu \cdot N$. In the scenario shown in Figure 1, we can use Hooke's law to derive an equivalent equation to describe the process of elastic deformation of a material under stress:

$$\delta F_c = E \cdot \varepsilon \cdot \delta s \tag{1}$$

In equation (1), E represents the elastic modulus, ε represents the dimensionless linear strain, δs is the micro-area of F_c , δf_c represents the micro-force of F_c , and F_c is the positive pressure produced by the peak value of R_z on claw teeth. In addition, S_0 is the sum of the effective shear-resistant areas of the surface δs . Based on these parameters, we can derive a functional relationship generated by F_c to compete with F_s , which can be expressed as follows:

$$\begin{aligned} F_s = F_a &= \int_0^{s_0} E \cdot \varepsilon \cdot \cos \theta \cdot d(s) \\ &= E \cdot \varepsilon \cdot \int_0^{s_0} \cos \theta \cdot d(s) \end{aligned} \tag{2}$$

(2) in the equation $\int_0^{s_0} \cos \theta \cdot d(s)$ is the shear area of the embedded agent.

In general, Ra value is an important factor in determining the shear resistance of the shear area of the surface. This is because the ratio of Ra to RZ will produce the effect of shear moment, which makes the surface shear strength proportional to the ratio of Ra to RZ. In other words, the magnitude of the surface shear strength is directly affected by the Ra/Rz ratio. See the expression:

$$\tau_{suf} \in \frac{R_a}{R_z} \tau_s \tag{3}$$

In the Formula τ_s is the shear strength of the material. Therefore, F_c can provide the force and F_s counterbalance, its clamp-in slippage force, and the material's elastic modulus and surface deformation area. Because it matters in the grand scheme of things:

$$F_c = \frac{N}{\sin(\theta)} \tag{4}$$

Thus, F_s is the product of the positive pressure N and the cotangent $\text{ctg}\theta$ of the wedge angle θ , where θ is closely related to the wedge angle of the roughness peak. Because the peak wedge angle is usually greater than the conventionally defined friction angle, the value of $\text{ctg}\theta$ is greater than the friction coefficient μ . When the claw teeth of the Tong body

contact with the steel wall of the pipeline under the N positive pressure, the combined force of slippage is produced by the embedded force and the surface contact friction force. See the following expression:

$$\begin{aligned} \overline{F_s} &= F_a + F_b \\ &= \alpha \cdot N \cdot ctg(\theta) + \beta \cdot \mu \cdot N \end{aligned} \tag{5}$$

This combined force is usually greater than friction alone, and sometimes much greater. In the above formula, α and β are the action distribution coefficients, the sum of which is equal to 1, that is, $\alpha + \beta = 1$. In addition, there is another situation to consider: when the positive pressure N is not enough to support the larger drag load F_s , claw teeth may slip down. In this case, the F_R force shown in Figure 1 is generated, which is a F_R friction force with the same coefficient of friction as the pure plane. It should be noted that the positive pressure that produces the F_R force comes from F_C . Therefore, we need to further analyze the effect of F_C on F_R forces, namely:

$$F_R = \mu \cdot F_C = \frac{\mu N}{\sin(\theta)} \tag{6}$$

Compared with the plane friction F_b ($F_b = \mu \cdot N$), the F_R force is significantly larger. By analyzing the mechanism of the embedded anti-skid, we can know that under the same positive pressure N , the embedded claw tooth can provide more climbing force for the robot. This is the significance of the claw-grip structure proposed by us. The slippage force produced by the structure in contact with the pipe steel wall is much larger than the friction force produced by simple plane contact.

In addition, this claw tooth design has another significant function. As some oil and water inevitably remain in the pipes, they can freeze over in the cold north. Due to the high-amplitude contact characteristic of claw teeth, it has a strong ice-breaking ability, which can ensure the reliable contact between claw teeth and pipe wall, and form stable adhesion, thus reducing the occurrence of skidding. The Claw tooth structure is as follows:

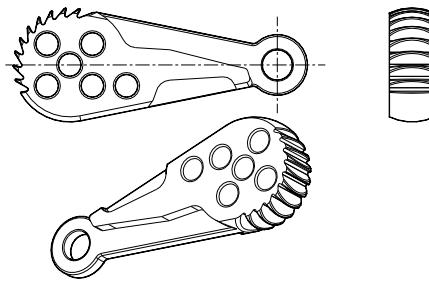


Figure 2. Structure of clamp body and claw tooth.

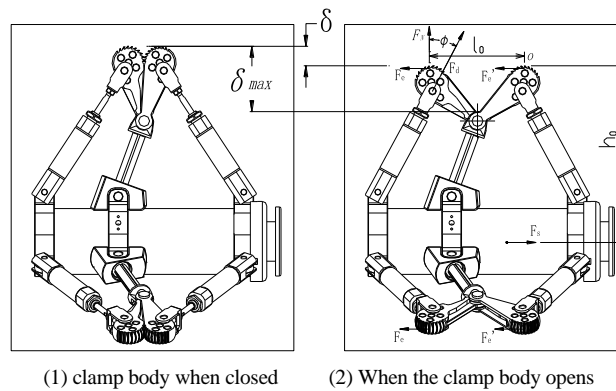


Figure 3. A grasping structure composed of two pincers.

From the above illustration, it is obvious that the claw-grip design has a wide design margin and excellent pipe diameter adaptability (that is, the ratio between the basic cylinder diameter D and the volumetric value δ). Therefore, it can adapt to different diameters of the pipeline, showing a wide range of adaptation, and its diameter-changing ability can even reach the maximum value of $2\delta_{max}$.

When the two clamp bodies are simultaneously in contact with the tube wall and act upon it, as shown in Figure 3(2). Therefore, we can regard it as a torque system with o -point as Fulcrum, and form a balance system which is composed of friction force system of six clamps. The equation for this equilibrium system can be expressed as follows:

$$\left\{ \begin{array}{l} 3(F_e + F_e') = F_s \\ F_e = \alpha \cdot F_N \cdot \text{ctg}(\theta) + \beta \cdot \mu \cdot F_N \\ F_e' = \mu \cdot F_N \\ F_N \cdot l_0 = F_s \cdot h_0 \\ F_N = F_d \cdot \cos \phi \end{array} \right. \quad (7)$$

According to the above equation, the strength of the clamp body and the maximum traction ability of the pipeline robot can be checked according to the above equation.

In addition, in order to solve the risk factors of sparks and static electricity that may be caused by friction between the forcepers and the pipeline, the occurrence of detonation incidents [3]. The pliers can be made of nylon, carbon fiber, and other polymer materials [4], as well as anti-static and wear-resistant materials such as ceramics [5]. If the body is made of steel, then its surface still needs to be coated with Teflon.

2. Webbed claw suction cup and its palatal pituitary columnar structure

2.1 Behavior analysis under force

For the crawling of plastic pipe, due to the smooth wall of the plastic pipe, its material often has a self-lubricating effect, so the clamp claw grip structure is no longer suitable for crawling in the pipe wall of the material. However, according to the characteristics of its soft plastic material and high surface density, it is very suitable for suction cup feet to walk reliably in its pipe wall. However, if the rubber is in contact with the surface of the plastic wall, its adsorption characteristics are also very poor. Therefore, this is put forward. The appearance of the model is as follows:

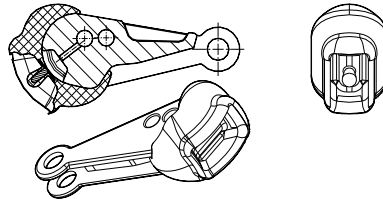


Figure 4. Schematic diagram of webbed claw sucker structure.

The outer lip of the webbed claw shown in the image above is in an arc to facilitate the removal of the positive pressure on the webbed claw. The front web is thicker, so that it can bear the load without excessive deformation and loss of suction, but the rear web is thinner, and its function is to play a sealing effect when the web claw is compressed and deformed, at the same time, when the positive pressure on the webbed claw is removed, the thin lip of the webbed claw can spring back and deform under the action of air pressure difference, so that the lip seam can be opened and air can enter into the sucker, thus the webbed claw can quickly leave the tube wall. In the cavity of the webbed sucker, there is a throat-tongue column. When the positive pressure acting on the webbed claw makes the webbed lip fully attach to the plastic pipe wall, the further increase of the positive pressure will make the column under pressure, and the volume of the cavity is increased so that the suction force can be generated and increased. Of course, for web-claw sucker cavity, increase its volume to improve its adsorption, but also can use “Diaphragm negative pressure method” and “Single flow discharge pressure method” and other design options, the “Diaphragm negative pressure method” can effectively block the damage of the forcepers body caused by the foreign body and the tumor in the pipeline, and prevent the foreign body from blocking the exhaust passage when the gas is discharged, see references [6, 7] for details. The process of loading is analysed as follows:

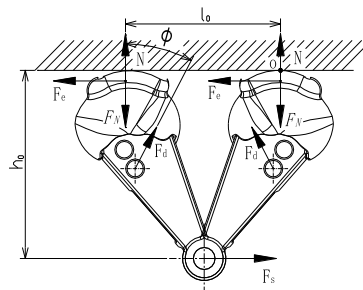


Figure 5. Sketch of Web Claw Force Analysis.

First of all, define the webbed claw material as the rubber material, which is through the cylinder or hydraulic cylinder to provide positive pressure N , so that its compression deformation and discharge of the gas cavity, resulting in a “Vacuum” adsorption, thus, the robot and the carrier are driven to walk. The suction is $F_N = S \times \Delta P / k$, where S is the sucker area, ΔP is the air pressure difference and K is the Factor of safety. Pressure differential calculation, as ideal gas law:

$$PV/T = nR \tag{8}$$

In the formula above, P is pressure, V is volume, T is absolute temperature, N is mole number and R is gas constant. Therefore, the pressure difference is:

$$\Delta P = P_1 - P_2 = T \cdot R \left(\frac{n_1}{V_1} - \frac{n_2}{V_2} \right) \tag{9}$$

Here P_1 is the atmospheric pressure and P_2 is the pressure inside the sucker after the webbed claw is compressed.

In formula (9), it can be seen that the role of the palatal pituitary column is to force the function of V_2 to increase. Of course, in addition to the throat-tongue column can make suction generated and increased, but also in the load, the rubber force due to the role of expansion, it is bound to increase the volume of its cavity V_2 , and the resulting pressure differential will increase again. Therefore, the webbed claw sucker structure has the following characteristics: the bigger the tangential load is, the more the suction force increases with the increase of the load.

If the self-weight of the robot is G , the load is W , the cylinder thrust is F_d , and the friction between the webbed claw and the plastic pipe wall is zero. Since there are three web fins acting on the wall of the plastic tube, the equilibrium equation is established according to Figure 5 with the O point as the Torque Center as follows:

$$\begin{cases} F_s = \frac{1}{3}(G + W) \\ F_N \cdot l_0 = F_s \cdot h_0 \\ F_N = F_d \cdot \cos \phi \end{cases} \tag{10}$$

It can be seen from equation (10) that the larger the distance between two webbed claws l_0 and the cylinder thrust F_d , the higher the load capacity, that is to say, the higher the resistance to F_s . In addition, when the webbed lips are compressed by the suction force of the webbed claws, the contact switch with the throat-tongue column is triggered to stop the suction, and according to the judgment of the central processor of the robot, whether the webbed lips continue to walk or not, according to the order of each leg and the foot posture, and then from the inhalation to a short-term exhaust process.

2.2 Balanced self-regulating cycle controlled pneumatic or hydraulic system

Because the structure of the robot is small and the load capacity is large, its control system should not have too many or too large auxiliary control devices and accessories. See below for a schematic diagram of the control mode of its pneumatic or hydraulic system:

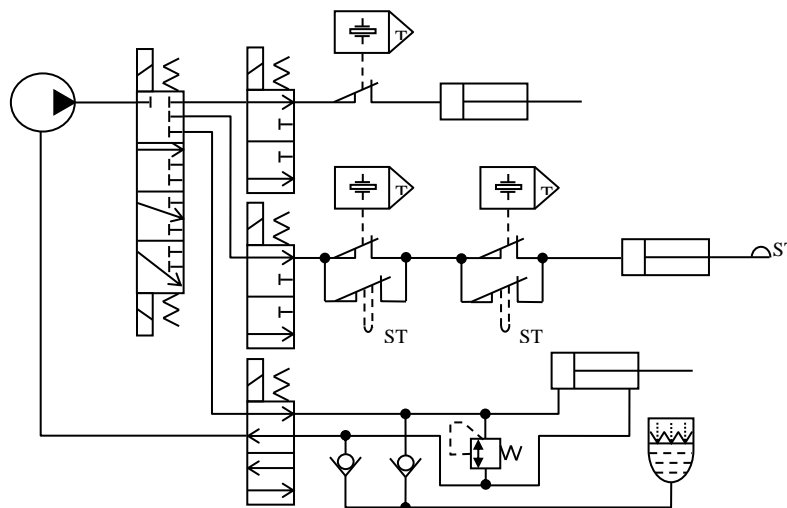


Figure 6. Simple schematic diagram of self-adjusting oil pressure circuit with double cylinder in-out hydraulic closed inner circulation balance (scheme 1).

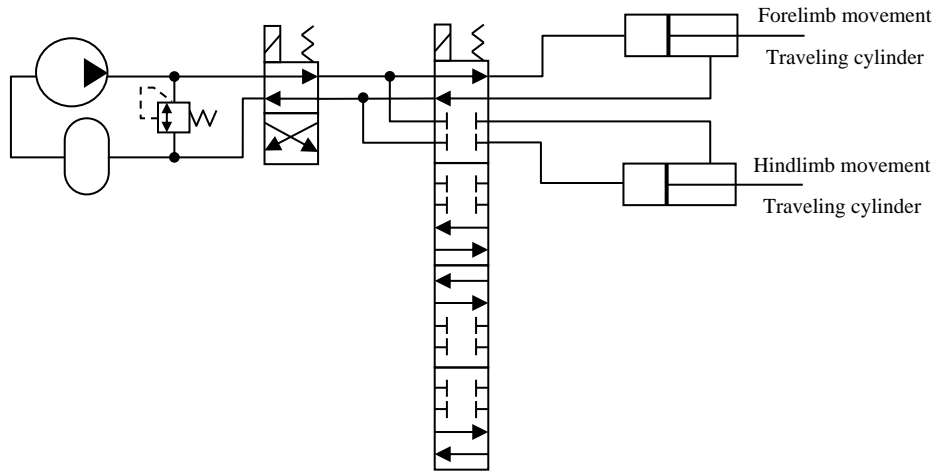


Figure 7. Simple schematic diagram of self-adjusting oil pressure circuit with double cylinder inlet and outlet air pressure closed internal circulation balance (scheme 2).

3. The structure of a clamped-in-pipe robot brief introduction

The core and basic components of the pipeline robot [2] are: 1 rudder; 2 rudder disk mechanism [8]; 3 clamp body gripping mechanism; 4 ankle two-dimensional soft hoof mechanism; 5 lumbar traction mechanism; 6 self-positioning fist gripping mechanism; 7 micro-probe mechanism, 8 direction retainer, 9 web-claw sucker body clamp mechanism and so on. According to the pipe diagram of memory, the network topology calculation is carried out reasonably. Therefore, it has good climbing, turning and obstacle climbing abilities, see the following figure:

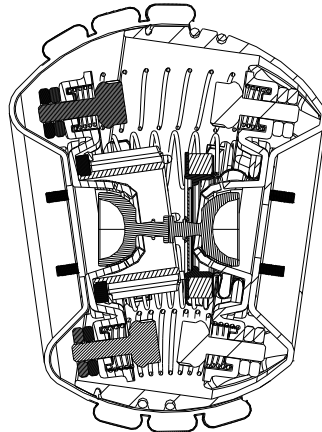


Figure 8. A diagram of the steering wheel separating when the robot turns.

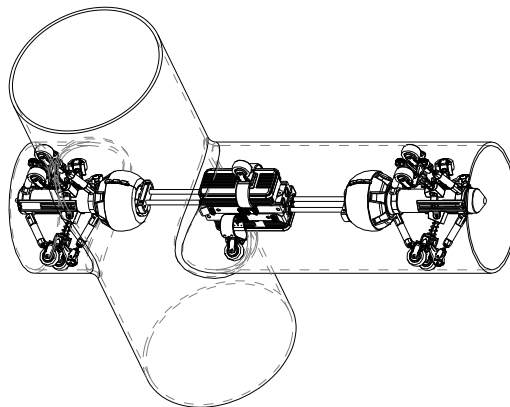


Figure 9. The action sketch of the rear limb overhang.

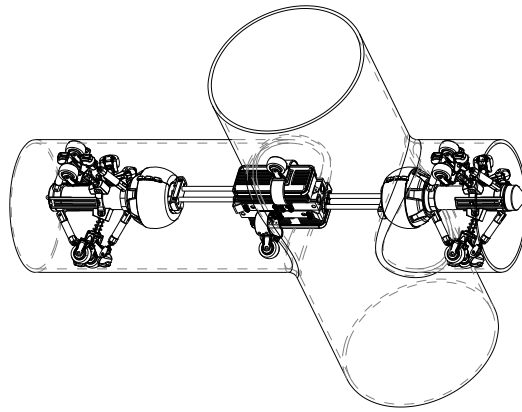


Figure 10. The action sketch of the forelimb overhang.

References

- [1] Research on Sui Seagull, a new type of flexible pipe-connected robot with abdominal wall [D]. Changzhou: Changzhou University, 2015.
- [2] Zhou Zhijing, Yin Gang, Chang Yung-hsiang. A vertical up-down pipe gripper robot [P]. Chinese patent: 202410252674.4, 2024-3.6.
- [3] Tan Guibin, Wang Dejie, Chen Yingchun. Tribology and reliability of deep-sea riser robot [J]. Petroleum mining machinery, 2016, 45(5): 88-96.
- [4] Lijin Liu. Study on anti-static technology of the Wu dynasty's Xuan, macromolecule material [J]. Technology Guide, 2014(20): 173.
- [5] Antistatic ceramic tile Gb26539-2011.
- [6] Zhou Zhijing, Yin Gang, Chang Yung-hsiang. A kind of rigid-hoofed web claw structure of pipeline robot [P]. Chinese patent: 202410133684.6, 2024-1-30.
- [7] Zhou Zhijing, Yin Gang, Chang Yung-hsiang. A kind of soft-hoofed web claw structure of pipeline robot [P]. Chinese patent: 202410131671.5, 2024-1-30.
- [8] Yin Gang, Chang Yung-hsiang, Lei Chuanmao. The utility model relates to a turning recognition and direction keeping mechanism of a pipe robot [P]. Chinese patent: 202311487593.4, 2023-11-9.